



1 Study on the measurement of isoprene by Differential Optical 2 Absorption Spectroscopy

3 Song Gao^{1,4}, Shanshan Wang^{1,2}, Chuanqi Gu¹, Ruifeng Zhang¹, Yanlin Guo¹, Yuhao
4 Yan¹, Bin Zhou^{1,2,3}

5 ¹Shanghai Key Laboratory of Atmospheric Particle Pollution and Prevention (LAP³), Department
6 of Environmental Science and Engineering, Fudan University, Shanghai 200438, China.

7 ²Institute of Eco-Chongming (IEC), No. 20 Cuinia Road, Shanghai 202162, China.

8 ³Institute of Atmospheric Sciences, Fudan University, Shanghai, 200433, China.

9 ⁴Shanghai Environmental Monitoring Center, Shanghai, 200235, China.

10 Corresponding author: Shanshan Wang (shanshanwang@fudan.edu.cn) and Bin Zhou
11 (binzhou@fudan.edu.cn)

12

13 **Abstract** In this paper, the continuous on-line measurements of isoprene in the
14 atmosphere have been carried out by using the Differential Optical Absorption
15 Spectroscopy (DOAS) in the band of 202.71–227.72 nm for the first time. Under the
16 zero optical path in the laboratory, different equivalent concentrations of isoprene
17 were measured by the combination of known concentration gas and series calibration
18 cells. The correlation between the measured concentrations and the equivalent
19 concentrations was 0.9996, and the slope was 1.065. The correlation coefficient
20 between DOAS and on-line VOCs instrument is 0.85 and the slope is 0.86 in the
21 comparison of 23 days field observation. It is estimated that the detection limit of
22 isoprene with DOAS is about 0.1 ppb at an optical path of 75 m, and it is verified that
23 isoprene could be measured in the ultraviolet absorption band using DOAS method
24 with high temporal resolution and low maintenance cost.

25 1. Introduction

26 Isoprene, named as 2-methyl-1,3-butadiene (C₅H₈), is an important BVOCs
27 (Biological Volatile Organic Compounds) in the atmosphere. Its global emission rate
28 is about 500 TgCyr⁻¹ (Sindelarova et al., 2014). Isoprene accounts for 70% of global
29 BVOCs emissions (Aydin et al., 2014). Land vegetation and other natural sources
30 contribute 90% of isoprene in the atmosphere (Zhang et al., 2016), and anthropogenic
31 emissions mainly come from industrial activities. Isoprene, as a typical pentadiene
32 hydrocarbon, has a higher activity than that of ordinary anthropogenic VOCs (Lian et



33 al., 2020), and its lifetime in the boundary layer is only about half an hour (Zheng et
34 al., 2015). Due to high volatility and reaction activity, isoprene can accelerate the
35 reaction between atmospheric substances, and it is easy to react with strong oxidizing
36 substances (OH, NO₃ radicals, etc.), and also affects the balance between NO_x (NO_x
37 = NO + NO₂) and O₃ in the atmosphere. Isoprene is also the precursor of secondary
38 organic aerosol (SOA) (Zeng et al., 2018).

39 Isoprene produced by plants is a byproduct of photosynthesis, its emission intensity
40 directly relates to the abundance of plants, leaf area index, and plant species.
41 Meteorological parameters, such as temperature, radiation intensity and humidity, can
42 also affect the emission of isoprene (Bai, 2015). In the daytime, the oxidation by OH
43 is the main chemical process of isoprene. Because of the existence of multiple double
44 bonds, the addition reaction with OH will lead to the formation of a variety of
45 products and the formation of RO₂. In the presence of NO_x, RO₂ can be further
46 reacted to convert RO and HO₂, causing the mutual conversion of free radicals and
47 the accumulation of ozone, which affects the balance of O₃ in the atmosphere.
48 Meanwhile, the reaction of isoprene with NO₃ mainly occurs at night. Although the
49 reaction only accounts for 6% - 7% of the total isoprene oxidation, it is an important
50 way to remove NO₃ (Xie et al., 2013).

51 In recent years, with the increase of urban vegetation diversity, the emission intensity
52 of urban BVOCs also has a significant upward trend. The monitoring and control of
53 isoprene in urban ecosystem has also attracted more and more attention. Because
54 isoprene concentration in the atmosphere is low, and the life time is short, high
55 precision and accuracy methods are needed for monitoring. Currently, general
56 methods, including gas chromatography-mass spectrometry (GC-MS), proton transfer
57 reaction mass spectrometry (PTR-MS), and chemical ionization mass spectrometry
58 (CIMS) et al. were introduced to measure the isoprene.

59 GC-MS is using the high separation ability of gas chromatography to separate the
60 components of environmental samples, and then measuring the different compounds
61 with the mass spectrometry. Although GC-MS has high precision and stability, it can
62 distinguish most VOCs qualitatively and quantitatively. But the complex requirements



63 in power, temperature control and special carrier gas make it is not easy in
64 maintaining and operating. GC-MS measurement generally requires sampling,
65 preservation and pre-treatment before analysis. During this process, the sample may
66 change to some extent, resulting in inaccurate results.

67 Proton-transfer reaction mass spectrometry (PTR-MS) is the chemical ionization of
68 gas sample through proton transfer in drift tube. The proton source is usually H_3O^+ .
69 The fixed length of the drift tube provides a fixed reaction time for the ions moving
70 along the drift tube, which makes the sample react with H_3O^+ continuously in the drift
71 tube to produce proton transfer, and then enter the mass spectrometer to screen
72 through the charge ratio. The disadvantage of PTR-MS is that it completely relies on
73 mass spectrometry to provide the identification of mixtures. VOCs as a class of
74 substances, it is possible to have the same molecular weight or the same mass of
75 fragment ions and parent ions. In this case, it is difficult to determine all species
76 present and their respective concentrations. A solution to this is to combine gas
77 chromatography (GC) with PTR-MS (Robert et al., 2009).

78 Chemical ionization mass spectrometry (CIMS) (Leibrock & Huey, 2000) retains the
79 qualitative ability of mass spectrometry, and coupling the traditional air sampler with
80 mass spectrometry technology. However, this method is not sensitive to low
81 concentration isoprene. In addition, the VOC composition in the atmosphere is
82 complex, and the unknown composition may react with benzene reagent to interfere
83 with the measurement results.

84 In addition, a portable gas chromatograph (iDirac) equipped with photo-ionization
85 detector to measure isoprene was proposed by Conor et al.(2020) in Cambridge
86 University. The instrument is an improved technology for GC-MS, which can work
87 independently weeks to months in the field environment. Previous studies rarely
88 mentioned the measurement of isoprene by spectral method. Brauer et al. (2014)
89 measured the infrared spectrum of isoprene by Fourier transform spectrometer, and
90 found that isoprene has a strong absorption near 11000nm, which provides a new
91 direction for the measurement of isoprene by spectral technology. So far, however,
92 few people have mentioned the measurement of isoprene by ultraviolet spectroscope.



93 In this paper, an on-line measurement method with high temporal resolution for
94 isoprene in the atmosphere is proposed by using the DOAS technology in the far
95 ultraviolet band.

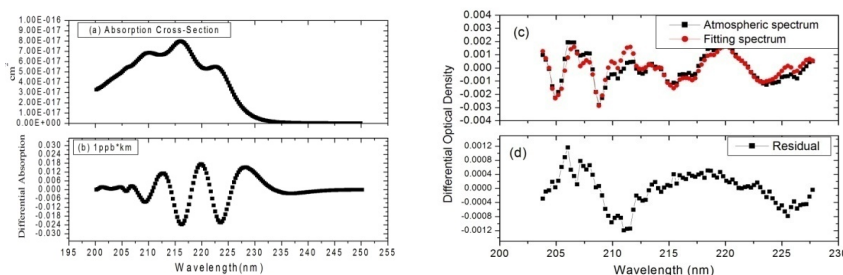
96 **2. Measurement method**

97 **2.1 Instrument introduction and spectral analysis**

98 DOAS technology was proposed by Platt et al. (1979, 1980) in 1970s for the first time.
99 The principle of the instrument was detailed in other literature (Platt & Stutz, 2008),
100 here is the description of deep UV-DOAS. The system is mainly composed of light
101 source, transmitting telescope, receiving telescope, spectroscopy, and computer, etc.
102 The transmitting and receiving telescopes are located at both ends of the measuring
103 optical path with a space of 75m. Since the measurement of isoprene is in deep
104 ultraviolet, we choose deuterium lamp (L6311-50, Hamamatsu, 35W) as light source,
105 the aperture of the transmitting telescope is 76mm, and the primary mirror is the UV
106 enhanced spherical mirror, while, the aperture of the receiving telescope is 152mm. A
107 spectroscopy (B&W TEK Inc. BRC741E-1024) with a spectral range of 185-400 nm,
108 a spectral resolution of 0.75 nm FWHM (Full Width Half Maximum), and a
109 1024-pixel photodiode array as detector was used to record spectrum. The
110 measurement routine is that the light emitted by the light source is collimated by the
111 transmitting telescope and then sent out, after a certain distance of transmission, it is
112 collected by the receiving telescope and focused on the incident end of the optical
113 fiber. The optical fiber feeds the light into the spectroscopy, which detects the light
114 signal and sends it to the computer for spectral analysis. The measured atmospheric
115 spectrum contains the absorption information of molecules in atmosphere. After
116 removing the Rayleigh scattering and Mie scattering, as well as the broadband
117 absorption of molecules by high pass filtering, the so-called differential absorption
118 spectrum is obtained. The concentration of the corresponding atmospheric
119 components can be retrieved by fitting differential absorption spectrum with the
120 differential absorption cross section of the measured molecules.
121 Isoprene has strong absorptions between 200.0-225.0nm, among which there are



122 relatively obvious absorption peaks (Martins et al., 2009) near 210.0nm, 216.0nm and
123 222.1nm, as shown in Figure 1a. After a 5th order polynomial fitting filtering, the
124 differential absorption spectrum (1ppb*km) of isoprene is shown in Figure 1b.
125 According to its differential absorption characteristics, the fitting band of isoprene is
126 202.71-227.72nm. Within this band, there are also absorptions of NH₃ (Chen et al.,
127 1999), SO₂ (Wu et al., 2000), NO, NO₂ (Mérieulle et al., 1995), C₆H₆ (Dawes et al.,
128 2017), C₇H₈ (Serralheiro et al., 2015), etc. The absorption of NO used here was
129 measured in laboratory with known concentration gas by using the same instrument.
130 Therefore, the absorption of these components is also considered in the process of
131 spectral retrieving. Figure 1c is an example of the spectrum fitting, the black line is
132 the actual atmospheric spectrum (2018-07-08 12: 47), while the red line is the fitting
133 spectrum (0.79ppb isoprene, 2.83ppb NH₃, 1.85ppb SO₂, 1.42ppb NO, 4.94ppb NO₂,
134 0.01ppb C₆H₆, 2.20ppb C₇H₈), and figure 1d is the fitting residual (standard deviation
135 is 4.76E-4).



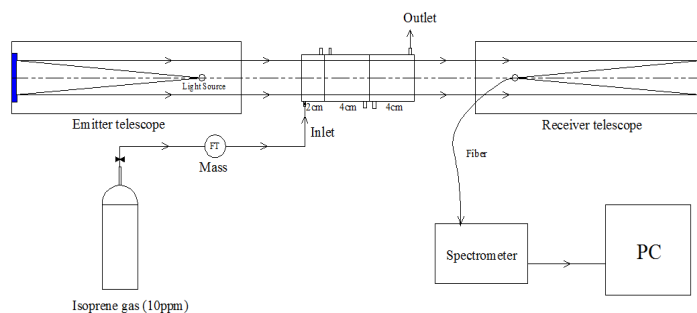
136
137 Figure1. The absorption Cross-section of isoprene(a), the differential absorption
138 spectrum of isoprene in 1ppb*km(b), the example of the spectrum fitting, the black
139 line is the actual atmospheric spectrum (2018-07-08 12: 47), and the red line is the
140 fitting spectrum (0.79ppb isoprene, 2.83ppb NH₃, 1.85ppb SO₂, 1.42ppb NO, 4.94ppb
141 NO₂, 0.01ppb C₆H₆, 2.20ppb C₇H₈) (c), the fitting residual (d)

142 2.2 Calibration experiment

143 In order to verify the accuracy of measurement results, isoprene gas with known
144 concentration is used to calibrate the instrument in the laboratory. The method is to
145 close the emitting telescope and receiving telescope (close to zero optical path) in the
146 laboratory, and then a series absorption cell was placed between the telescopes.



147 10ppm isoprene gas was injected into the cells at a constant flow rate of 100ml/min,
 148 and then the corresponding concentration under different cell combinations was
 149 measured, as shown in Figure 2.



150

151 Figure 2. The scheme of the calibration system

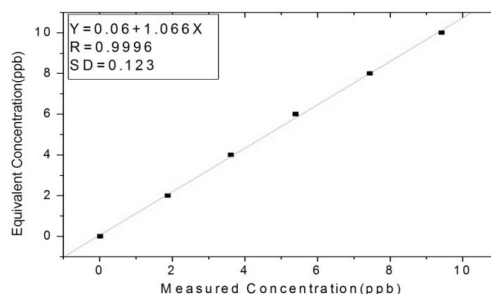
152 The absorption cell group is composed of one 2cm and two 4cm long cells in series.
 153 When using different combination of cells, different equivalent concentrations
 154 (C_E)(equivalent to the average concentration in the 100m optical path) can be
 155 obtained. The specific combination and corresponding equivalent concentrations, as
 156 well as the actual measurement concentrations (C_M) are shown in table 1.

157 Table 1: the calibration results in different gas cells combination

Length of cells	C_E (ppb)	C_M (ppb)
empty	0	0.01
2cm	2.00	1.88
4cm	4.00	3.61
2cm+4cm	6.00	5.40
4cm+4cm	8.00	7.44
2cm+4cm+4cm	10.00	9.42

158 Fig. 3 is the linear fitting of calibration results. The ordinate in the figure is the
 159 equivalent concentration, and the abscissa is the measured concentration. For six
 160 measuring points including the zero point, the linear fitting correlation coefficient R is
 161 0.9996. The relationship between the equivalent concentration and the measured
 162 concentration is shown in the following equation (1). For the future measurement
 163 results of the actual atmosphere, equation (1) will be used to calibrate the measured
 164 data.

165
$$C_E = 0.06 \text{ppb} + 1.066 * C_M \quad (1)$$



166

167 Figure3. The linear fitting of calibration results, the ordinate is the equivalent
168 concentration and the abscissa is the measured concentration

169 3. Field comparison experiment and discussion

170 3.1 Comparison with on-line VOCs results

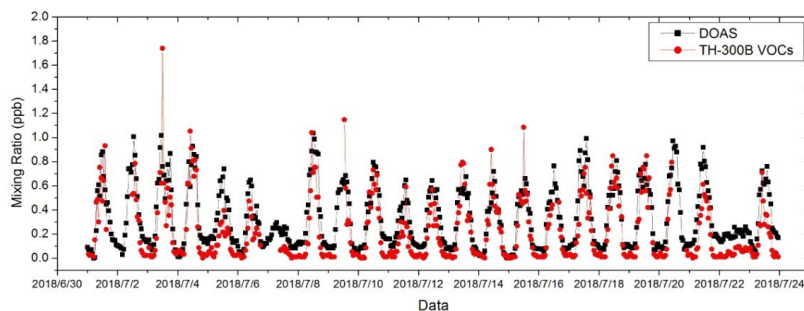
171 In order to further verify the reliability of DOAS method in actual atmospheric
172 measurement, in July 2018, the field measurement results of the DOAS were
173 compared with the on-line VOCs (TH-300B on-line VOCs monitoring system)
174 analyzer (Zhu et al., 2020), which is based on the GC-MS technology. DOAS
175 instrument is installed on the 7th floor of the Environmental Science Building
176 (31.344 ° N, 121.518 ° E) in Jiangwan campus of Fudan University, as shown in
177 Figure 4. The optical path is about 25m above the ground. The transmitting telescope
178 is at the west part of the building (A in Figure 4), while the receiving telescope is at
179 the east part (B in Figure 4). The distance between the telescopes is 75m. The on-line
180 VOCs instrument is located in Xinjiangwan City monitoring station of Shanghai
181 Environmental Monitoring Center (C in Figure 4). The straight-line distance is about
182 0.5km to the south of DOAS instrument. The coverage rate of plants around the
183 observation sites is high, mainly including pine, camphor, etc., and a large number of
184 lawns are also distributed. Meteorological parameters were recorded by the automatic
185 weather station (CAMS620-HM, Huatron Technology Co. Ltd) co-located with DOAS
186 instrument.



187

188 Figure4. Field measurement sites of DOAS and on-line VOCs, A is the transmitting
189 telescope, B is the receiving telescope, and C is the on-line VOCs, the yellow arrow is
190 light path of DOAS. This map is sourced from © Baidu

191 The comparison experiment was carried out from July 1st to 23rd, 2018. The temporal
192 resolution of DOAS was 1 min, while that of on-line VOCs was 1 h. In order to make
193 a good comparison, DOAS data were averaged hourly. Figure 5 shows the time series
194 of the data. It can be seen that the measurement results of the two instruments are in
195 good agreement. The average values of DOAS and on-line VOCs were 0.325ppb and
196 0.217ppb, and the standard deviation (SD) was 0.254ppb (N=551) and 0.257ppb
197 (N=466), respectively. The average value of DOAS results is higher than on-line
198 VOCs mainly because, at night, DOAS can still detect a certain concentration in most
199 cases, most of which are between 0.02-0.1ppb, while most of on-line VOCs data are
200 between 0-0.05ppb. Since the observation is in summer, there is also a very high
201 temperature at night during the observation period, i.e. 27.1°C (19:00-06:00 next
202 morning). In addition, the release of isoprene produced by the leaves of plants in the
203 daytime is delayed to some extent, resulting in a certain concentration of isoprene
204 remaining at night, so that we think the data of DOAS is more reasonable.



205

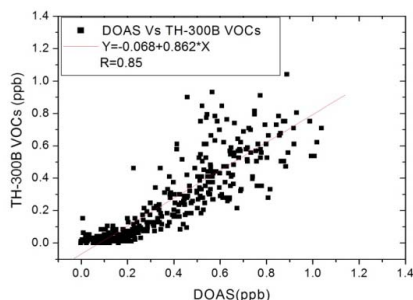
206 Figure 5. Time series data of DOAS and on-line VOCs measured isoprene during the
207 comparison measurement

208 Due to the missing of some data of on-line VOCs during the comparison period,
209 totally 466 sets of hourly data were used to analyze the correlation between these two
210 instruments. As shown in Figure 6, the correlation coefficient is 0.85 and the slope is
211 0.86. The main reason for the difference of DOAS and on-line VOCs results is that
212 the sampling and measurement heights of the two instruments are different. The light
213 path of DOAS is about 25m above the ground, while the sampling height of on-line
214 VOCs instrument is about 10m. Isoprene will rise up and diffuse after emission from
215 plants, so higher measurement points will catch higher concentration of isoprene. In
216 addition, the sampling of on-line VOCs is through the sampling tube, and isoprene
217 will be more or less lost during the sampling process. Those two reasons will
218 eventually lead to DOAS measurement results higher than online VOCs instruments,
219 especially when the isoprene concentration is very low at night, the difference is more
220 obvious.

221 It can also be seen from Figure 6 that when the isoprene concentration is higher than
222 0.5ppb, the measurement results of the two instruments show large scattering. The
223 main reason is that the spatial distance between the two instruments is about 500m,
224 considering the inhomogeneity spatial distribution of isoprene, this spatial difference
225 will lead to different data results between two instruments. Meanwhile, there are
226 various vegetations between the instruments, when the wind direction changes, the
227 emission of this part of vegetation will also cause the difference between the results of



228 the instruments. The different measurement principles, especially the difference of
229 sampling time can also cause the scattering of the results of two instruments. On-line
230 VOCs only has about 50% of the time (1h) to be used to sampling, while the rest of
231 the time is used for analysis. But DOAS is almost continuous measurement with just a
232 little part of time to be used for analysis (about 1s per minute), this difference will
233 affect the consistency of results. But in general, DOAS and on-line VOCs analyzers
234 show a good agreement in the comparison of mean and correlation of measured data.



235

236 Figure6. The correlation between DOAS and on-line VOCs instruments during the
237 field measurement

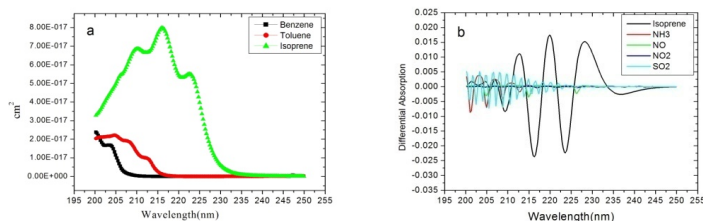
238 3.2 Detection limit evaluation

239 The detection limit of DOAS mainly depends on the signal-to-noise ratio of the
240 spectrum. Under the condition of zero light path in the laboratory, the zero noise
241 (standard deviation of the results) of isoprene is 0.007ppb, the detection limit can be
242 definite as two times of zero noise, so that the detection limit of the system is
243 0.014ppb (HJ 654-2013). However, in the real atmospheric measurement, it is
244 difficult to determine the actual detection limit due to the varied environment and the
245 interference of other gases. The detection limit of DOAS in real atmosphere is mainly
246 determined by the residual of spectral fitting. The residual mainly comes from the
247 absorption of interfering substances, the change of lamp spectral intensity and
248 structure, the spectral shift caused by the change of ambient temperature of the
249 spectrometer, and the noise of the detector. In order to reduce the influence of these
250 factors on the measurement, in the process of spectra fitting, the absorption of
251 interfering substances and the spectral structure of lamp are necessary to be



252 considered together with the isoprene. At the same time, it is also necessary to
253 calibrate the spectral drift. However, there are still some residual remain after the
254 spectral fitting.

255 In the fitting band of isoprene, the absorption of NO, benzene and toluene are the
256 main interference factors. The reason for the influence of NO is that there are three
257 obvious absorption peaks of NO in the fitting band. After high pass filtering, there is
258 component in the differential absorption cross section of NO similar to the variation
259 frequency of isoprene's differential absorption spectrum. After the analysis of the
260 measurement results, the impact of NO on isoprene is about 0.3% of its concentration.
261 But the effect of NO is mainly in the morning and evening rush hour. The influence of
262 benzene and toluene is mainly due to their strong absorptions in the fitting band of the
263 spectrum. Their presence will lead to a significant reduction in the spectral intensity in
264 the band, resulting in a reduction in the signal-to-noise ratio of the spectrum. During
265 the comparison experiment, high concentration of benzene or toluene occasionally
266 occurs, resulting in a large fitting residual. Other aromatics, such as xylene and
267 styrene, also absorb strongly in the fitting band, but because of their lower
268 concentration in the natural atmosphere, their impacts on isoprene are significantly
269 smaller than that of benzene and toluene. Although NH₃, SO₂ and NO₂ have
270 absorption in the fitting band, their differential absorption variation frequency is
271 significantly higher than that of isoprene, and only overlaps in parts of fitting band, so
272 that they have little influence on the isoprene measurement. Fig. 7a is the absorption
273 cross section of benzene, toluene and isoprene, while Fig. 7b is the differential
274 absorption spectra (1ppb*km) of NO, SO₂, NO₂, NH₃ and isoprene.



275

276 Figure 7. The absorption cross section of benzene, toluene and isoprene (a), the



277 differential absorption spectra ($1\text{ppb}\cdot\text{km}$) of NO, SO₂, NO₂, NH₃ and isoprene (b)
278 Whether it is benzene, toluene, or NO, SO₂, NO₂ and NH₃, they all exist together with
279 isoprene in the atmosphere. Therefore, their influences on isoprene measurement are
280 common. In order to ensure the quality of results, the data with a residual of more
281 than 0.0005 are filtered out. In a total of 33120 sets of data during 23 days observation,
282 1137 sets are filtered out, and the valid rate of data is 96.6%. The average residual of
283 all valid data is 0.000234. In order to evaluate the detection limit of DOAS in the real
284 atmospheric measurement, we made a statistic on 16387 sets of data with the
285 concentration of isoprene lower than 0.1ppb (assuming that the isoprene in the
286 atmosphere is close to zero at this time), and the standard deviation is 0.0499ppb, so
287 the detection limit of DOAS instrument in the field measurement is no more than
288 0.1ppb (twice the standard deviation).

289 **4. Conclusion**

290 This paper introduces, for the first time, the continuous on-line measurement of
291 isoprene in the atmosphere by means of DOAS in the band of 202.71-227.72nm.
292 Although the current measurements of isoprene are mainly GC-MS, PTR-MS and
293 CIMS methods, The DOAS method has the characteristics of high time resolution,
294 rapid temporal response and simple operation. It is especially suitable for long-term
295 online measurement in the field or forest where the traffic is inconvenient, and the
296 low cost of instrument is also conducive to build monitoring network.
297 Under the condition of zero optical path in the laboratory, several equivalent
298 concentrations were measured by using a series absorption cell and known
299 concentration of isoprene gas. The correlation coefficient between the measured
300 concentration and the equivalent concentration was 0.9996, and the slope was 1.065,
301 indicating that the instrument has good linearity and accuracy. After 23 days of field
302 comparison, there is a good correlation between the results of DOAS and on-line
303 VOCs instrument, with a correlation coefficient of 0.85 and a slope of 0.86.
304 Considering the different measurement principles, the different measurement
305 environment and the space distance between them, the comparison results shows a



306 good agreement between the two instruments.
307 In order to evaluate the detection limit of DOAS instrument under the actual
308 atmospheric measurement, the paper proposes to calculate the standard deviation of
309 all the data when the measured concentration of isoprene in the ambient air is close to
310 zero ($< 0.1\text{ppb}$, $n = 16387$). It is estimated that the detection limit of the DOAS is no
311 more than 0.1ppb under a measurement light path of 75m. Therefore, the DOAS is
312 suitable for long-term monitoring in cities or areas with large vegetation coverage.

313

314 **Data availability.** Data are published as [https:// DOI: 10.17632/489mvgbsxg.3](https://doi.org/10.17632/489mvgbsxg.3)

315 **Author contribution.** The study was designed by SG and BZ. Experiments were
316 performed by YG, RZ and YY. Data processing and analysis were done by BZ and
317 CG. The paper was written by BZ , SW and SG.

318 **Competing interests.** The authors declare that they have no conflict of interest.

319 **Acknowledgements.** This research has been supported by the National Key Research
320 and Development Program of China (grant No. 2016YFC0200401and
321 2017YFC0210002), the National Natural Science Foundation of China (grant No.
322 21777026, 41775113 and 21976031).

323

324 Reference

- 325 Aydin, Y. M., Yaman, B., Koca, H., Dasdemir, O., Kara, M., Altioek, H., et al. (2014). Biogenic
326 volatile organic compound (BVOC) emissions from forested areas in Turkey: determination of
327 specific emission rates for thirty-one tree species. *Science of the Total Environment*, 490,
328 239-253.<https://doi.org/10.1016/j.scitotenv.2014.04.132>
- 329 Bai, J. (2015). Estimation of the isoprene emission from the Inner Mongolia grassland.
330 *Atmospheric Pollution Research*, 6(3), 406-414.<https://doi.org/10.5094/APR.2015.045>
- 331 Blake, R. S., Monks, P. S., & Ellis, A. M. (2009). Proton-Transfer Reaction Mass Spectrometry.
332 *Chemical Reviews*, 109(3), 861–896.<https://doi.org/10.1021/cr800364q>
- 333 Brauer, C. S., Blake, T. A., Guenther, A. B., Sharpe, S. W., Sams, R. L., & Johnson, T. J. (2014).
334 Quantitative infrared absorption cross sections of isoprene for atmospheric measurements.
335 *Atmospheric Measurement Techniques*, 7(11),
336 3839-3847.<https://doi.org/10.5194/amt-7-3839-2014>
- 337 Chen, F. Z., Judge, D. L., Wu, C. Y. R., & Caldwell, J. (1999). Low and room temperature
338 photoabsorption cross sections of NH_3 in the UV region. *Planetary and Space Science*, 47,
339 261-266.[https://doi.org/10.1016/S0032-0633\(98\)00074-9](https://doi.org/10.1016/S0032-0633(98)00074-9)
- 340 Conor, G. B., Valerio, F., Andrew, D. R., Mohammed, I. M., Mohd, S. M. N., John, A. P., et



- 341 al.(2020). iDirac: a field-portable instrument for long-term autonomous measurements of
342 isoprene and selected VOCs. *Atmospheric Measurement Techniques*, 13, 821-838.
343 <https://doi.org/10.5194/amt-13-821-2020>
- 344 Dawes, A., Pascual, N., Hoffmann, S. V., Jones, N. C., & Mason, N. J. (2017). Vacuum ultraviolet
345 photoabsorption spectroscopy of crystalline and amorphous benzene. *Physical Chemistry
346 Chemical Physics*, 19, 27544-27555. <https://doi.org/10.1039/c7cp05319c>
- 347 HJ 654-2013, Specifications and Test Procedures for Ambient Air Quality Continuous Automated
348 Monitoring System for SO₂, NO₂, O₃ and CO, national standard of China, 2013.
349 http://www.cnemc.cn/jcgf/dqhj/201711/t20171108_647283.shtml
- 350 Leibrock, E., & Huey, L. G. (2000). Ion chemistry for the detection of isoprene and other volatile
351 organic compounds in ambient air. *Geophysical Research Letters*, 27(12),
352 1719-1722. <https://doi.org/10.1029/1999GL010804>
- 353 Lian, H. Y., Pang, S. F., He, X., Yang, M., Ma, J. B., & Zhang, Y. H. (2020). Heterogeneous
354 reactions of isoprene and ozone on alpha-Al₂O₃: The suppression effect of relative
355 humidity. *Chemosphere*, 240, 124744. <https://doi.org/10.1016/j.chemosphere.2019.124744>
- 356 Martins, G., Ferreira-Rodrigues, A. M., Rodrigues, F. N., de Souza, G. G. B., Mason, N. J., Eden,
357 S., et al. (2009). Valence shell electronic spectroscopy of isoprene studied by theoretical
358 calculations and by electron scattering, photoelectron, and absolute photoabsorption
359 measurements. *Physical Chemistry Chemical Physics*,
360 11, 11219-11231. <https://doi.org/10.1039/B916620C>
- 361 Mérienne, M. F., Jenouvrier, A., & Coquart, B. (1995). The NO₂ absorption spectrum. I:
362 Absorption cross-sections at ambient temperature in the 300-500 nm region. *Journal of
363 Atmospheric Chemistry*, 20(3), 281-297. <https://doi.org/10.1007/BF00694498>
- 364 Platt, U., Perner, D., Harris, G. W., Winer, A. M., & Pitts, J. N. (1980). Detection of NO₃ in the
365 polluted troposphere by differential optical absorption. *Geophysical Research Letters*, 7,
366 89-92. <https://doi.org/10.1029/GL007i001p00089>
- 367 Platt, U., Perner, D., & Pätz, H. W. (1979). Simultaneous measurement of atmospheric CH₂O, O₃,
368 and NO₂ by differential optical absorption. *Journal of Geophysical Research: Oceans*, 84(C10),
369 6329-6335. <https://doi.org/10.1029/JC084iC10p06329>
- 370 Platt, U., & Stutz, J. (2008). *Differential Optical Absorption Spectroscopy-Principles and
371 Applications*. Springer.
- 372 Serralheiro, C., Duflo, D., Ferreira, F. da Silva, Hoffmann, S. V., Jones, N. C., Mason, N. J., et
373 al. (2015). Toluene valence and Rydberg excitations as studied by ab initio calculations and
374 vacuum ultraviolet (VUV) synchrotron radiation. *The journal of physical chemistry. A*, 119,
375 9059-9069. <https://doi.org/10.1021/acs.jpca.5b05080>
- 376 Sindelarova, K., Granier, C., Bouarar, I., Guenther, A., Tilmes, S., Stavrakou, T., et al. (2014).
377 Global data set of biogenic VOC emissions calculated by the MEGAN model over the last 30
378 years. *Atmospheric Chemistry and Physics*, 14(17),
379 9317-9341. <https://doi.org/10.5194/acp-14-9317-2014>
- 380 Wu, C. Y. R., Yang, B. W., Chen, F. Z., Judge, D. L., Caldwell, J., & Trafton, L. M. (2000).
381 Measurements of high-, room-, and low-temperature photoabsorption cross sections of SO₂ in
382 the 2080- to 2950-Å region, with application to Io. *Icarus*, 145,
383 289-296. <https://doi.org/10.1006/icar.1999.6322>
- 384 Xie, Y., Paulot, F., Carter, W. P. L., Nolte, C. G., Luecken, D. J., Hutzell, W. T., et al. (2013).



- 385 Understanding the impact of recent advances in isoprene photooxidation on simulations of
386 regional air quality. *Atmospheric Chemistry and Physics*, 13(16),
387 8439-8455. <https://doi.org/10.5194/acp-13-8439-2013>
388 Zeng, Y., Shen, Z., Zhang, T., Lu, D., Li, G., Lei, Y., et al. (2018). Optical property variations from
389 a precursor (isoprene) to its atmospheric oxidation products. *Atmospheric Environment*, 193,
390 198-204. <https://doi.org/10.1016/j.atmosenv.2018.09.017>
391 Zhang, X., Huang, T., Zhang, L., Shen, Y., Zhao, Y., Gao, H., et al (2016). Three-North Shelter
392 Forest Program contribution to long-term increasing trends of biogenic isoprene emissions in
393 northern China. *Atmospheric Chemistry and Physics*, 16(11),
394 6949-6960. <https://doi.org/10.5194/acp-16-6949-2016>
395 Zheng, Y., Unger, N., Barkley, M. P., & Yue, X. (2015). Relationships between photosynthesis and
396 formaldehyde as a probe of isoprene emission. *Atmospheric Chemistry and Physics*, 15(15),
397 8559-8576. <https://doi.org/10.5194/acp-15-8559-2015>